Systematic Deviations Between Theoretical and Experimental EXAFS Functions; Possible Evidence of Interstitial Scattering Outside the Muffin-tin Radius in EXAFS Spectra

Z. Kvitky[1], F. Bridges[2], G. van Dorssen[3]
[1] *Stanford Linear Accelerator Center, Menlo Park, CA*
[2] *Physics Department, University of California, Santa Cruz, CA 95064*
[3] *Philips Analytical, 5600 MD Eindhoven, The Netherlands*
(Draft: October 9, 2001)

EXAFS analysis utilizing theoretical standards generated by the FEFF6 and FEFF7 codes often suffer from small systematic deviations on the high-r side of the first neighbor peak in the Fourier transform. Similar deviations may also occur for other codes that are based on nonself-consistent muffin-tin potentials. These deviations substantially decrease the goodness of fit, and in more complex crystal systems which have more than one peak in the first neighbor shell, may change the resulting fit parameters significantly. We have carefully investigated four simple systems: Ag, Au, Pb, and RbBr, each of which has only one bond length in the first neighbor shell. Fits using theoretical functions show deviations on the high-r side of the peak; in k-space, the problem is associated with structure in the effective backscattering amplitude function F(k), calculated by FEFF, particularly in the low-k region below 8Å^{-1}. We compare the fits obtained using FEFF functions and experimentally determined EXAFS standards. The deviations on the high-r side of the first peak are important for an accurate analysis of complex materials with several closely spaced neighbors or systems with distorted local environments, because such differences may be mistaken for additional or displaced neighbors. This is illustrated by fitting the first Ag-Ag shell for Ag metal to a sum of two peaks. A good fit can be achieved, but yields the unphysical result that a few long Ag-Ag bonds at 3.15 Å exist. Models to date are based on the spherical muffin-tin approximation which ignore the non-sphericity of the true potential about each atom and treat the interstitial region as a constant potential outside the muffin-tin radii. To crudely include some anisotropy we have used H atoms at interstitial sites as a surrogate for scattering in the interstitial region and show that an additional peak occurs at exactly the region in r-space where the deviation between FEFF and experimental data is largest for Ag.

Keywords: XAFS, FEFF

I. INTRODUCTION

Over the past twenty years, the Extended X-Ray Absorption Fine Structure (EXAFS) technique has become an increasingly powerful method of analyzing local structure in a wide variety of materials.[1,2] The oscillations in X-ray absorption which result from interference between the outgoing photoelectron wave from the absorbing atom and backscattered waves from surrounding atoms can be analyzed to extract information about number of neighboring atoms, their distance from the absorber, amplitudes of thermal vibration, and anharmonicity in atomic bonds. Because EXAFS is directly connected in this manner with local structure, it has become widely used to study dilute and amorphous systems (liquids, suspensions, nanocrystals, proteins, coordination number and valence of dilute toxins in soil and water samples) that cannot be easily examined through alternate experimental techniques.

Analysis is typically undertaken by performing a least-squares fit between data and any number of EXAFS atom-pair standards, which may be either experimentally derived or theoretically generated. Parameters expressing number of neighbors, atom-pair distances, pair distribution width, and anharmonicity are varied to achieve reasonable fits, and determine the local structure around the absorber. The goodness of fit and accuracy of structural parameters is thus dependent on the quality of the standards used in fitting. Experimentally determined standards can be derived from EXAFS data taken at low temperatures using model compounds which have simple, well-characterized structures. Such model compounds, however, are not always available. Theoretical standards can be easily generated with an EXAFS simulation code such as FEFF[3] (FEFF6.01a was used in much of this study; FEFF 7.02 calculations yielded similar results in several tests) for any cluster of atoms at a given temperature, and are thus far easier to obtain than experimental ones. Indeed, FEFF is very widely used in EXAFS analysis and has been shown to provide excellent agreement with experimental data.[4] As this study will show, however, there persist some systematic deviations in FEFF-generated standards that can significantly worsen the quality of fits, and produce small but sometimes significant errors in extracted fit parameters. We expect that similar deviations exist for other theoretical codes that are base on nonself-consistent muffin-tin potentials, but have not verified this possibility.

Only simple materials with well-characterized crystal structures were utilized in the study: Ag, Au, and Pb foils, and a powdered sample of RbBr. The original motivation for analysis of such simple compounds was to attempt to extract information about $U(r - r_0)$, the atom-pair potential for the nearest neighbor(s).[5] It was found that both fit quality and extracted potential pa-

rameters were highly sensitive to the range in r-space over which the data were fit, with the best and most consistent fits for the potential model being those carried out over a very wide range in r-space using experimental standards for the first peak. These materials all have a well-separated first neighbor shell with only a single bond-length, and were therefore excellent candidates for such a study. Despite excellent separation of transformed peaks, a problem was encountered when the fit range was extended even a small distance beyond the half height point of the first peak on the high-r side if FEFF functions were used; the quality of fit proved to worsen very rapidly.

Deviations between FEFF standards and the data are found to systematically occur on the high-r side of the Fourier transformed peak for all samples studied, and therefore require that fits be conducted over a shorter r-range than would otherwise be desired to obtain a good fit. Inclusion of this high-r region always decreases the goodness of fit parameter when using FEFF functions, often by a factor > 4, and can sometimes lead to significant errors in fit parameters when there is more than one peak in the first shell. Analysis shows that these discrepancies are mainly related to apparent errors in the calculated amplitude function for the backscattered wave as a result of the assumptions used in FEFF (and other similar multiple scattering codes); they occur primarily in the low to mid-k region, below 8Å^{-1}. One possibility is that as a result of using muffin-tin potentials (with a spherical potential used for each atom out to the muffin-tin radius), the FEFF calculation does not take into account the anisotropy of the real potential (particularly near the muffin-tin radius) or variations of the potential in the interstitial regions. The difference between the muffin-tin potential and a more realistic potential will include non-spherical atom effects and a varying interstitial potential. We crudely model the scattering from this difference potential by placing H or other atoms at an interstitial site to produce additional scattering from the interstitial region. Our simulations suggest that such scattering may explain the discrepancies between the FEFF calculations and the experimental data. However, we cannot rule out the possibility that other approximations made in the FEFF calculations produce these discrepancies.

Section II describes the experimental setup and data acquisition, Section III outlines the methods of data extraction and analysis undertaken to obtain the EXAFS functions presented, while Section IV presents the results for the extracted parameters and the goodness of fit. Section V provides a discussion and comparison of these results.

II. SAMPLES AND EXPERIMENTAL METHODS

All data presented here were collected at station 9.2 at the Daresbury Synchrotron source in Daresbury, England, using a monochromator with Si(220) crystals. Measurements were carried out in a He cryostat with mylar windows installed on either side to allow X-ray transmission through the enclosed sample. Gas ionization detectors on either side of the cryostat were used to collect absorption data. Temperatures down to 15K were attainable for data measurement, with the samples covered by thin Al foil in contact with the cold finger to ensure temperature uniformity across the sample. The energy resolution varies from 2-4eV as shown in Table I, depending on the X-ray energy and the vertical height of the beam.

Gold, silver, and lead foils were examined, as was a sample of RbBr, which was prepared by brushing a fine powder onto scotch tape. The RbBr EXAFS sample consisted of four such double layers of tape to give a thickness of approximately one absorption length. The foils used have thicknesses of 1-3 absorption lengths.

III. BACKGROUND SUBTRACTION AND DATA ANALYSIS

A. Data Reduction

In order to extract the EXAFS oscillations from the absorption curve, a smooth curve consisting of several cubic splines is fit to the data such that it roughly intersects the midpoint of each oscillation. Since the "free-atom" absorption is unknown, there is some ambiguity in selecting an appropriate smooth background function, but care is taken to avoid removing EXAFS oscillations during this removal process[4,6]. We assume to this end that this background function, $\mu_0(E)$, is smooth, and that the average value of $\chi(k)$ over most of its transformed range is zero. The spline fit typically begins at an energy 15-30eV above E_0, the edge energy at half height. This background function is then subtracted and used to normalize the data via the relation

$$\chi(E) = \frac{\mu(E) - \mu_0(E)}{\mu_0(E)}$$

where $\mu_0(E)$, the "embedded atom" absorption[7], is the part of $\mu(E)$ without EXAFS oscillations. Setting the momentum of the ejected photoelectron to zero at E_0, the wave number can be expressed as

$$k = \sqrt{\frac{2m}{\hbar^2}(E - E_0)}. \quad (1)$$

This is used to convert $\chi(E)$ to $\chi(k)$. For the case of N_i identical atoms at a given distance, r_i, from the absorbing atom, χ_i can then be expressed as a sum of terms of the form

$$\chi_i(k) = Ae^{\frac{-2\Delta r_i}{\lambda_i}} e^{-2k^2\sigma_i^2} sin\left(2k(r_{0_i} + \Delta r_i) + \Phi(k)\right) \quad (2)$$

$$A = \frac{N_i S_{0_i}^2 F_i(k)}{k r_{0_i}^2} \tag{3}$$

$$\Phi(k) = -4k\sigma_i^2 \left(\frac{1}{r_{0_i}} + \frac{1}{\lambda}\right) - \frac{4}{3} C_{3_i} k^3 + \phi_i(k) \tag{4}$$

when σ_i, and C_{3_i} are not too large. In Eqn. 3, N_i is the number of neighbors at a distance $r_{0_i} + \Delta r_i$ (r_{0_i} is the starting value) from the absorber, $S_{0_i}^2$ is an amplitude reduction factor to account for multi-electron processes which diminish the EXAFS signal, $F_i(k)$ and $\phi_i(k)$ are the effective backscattering amplitude (which includes a mean free path term exp(-2r_{0_i}/ λ_i)) and the total phase shift, both of which are calculated by the FEFF6,7 code[3]. λ is the average mean free path (8Å), σ_i is the Debye-Waller factor, and the third cumulant (C_{3_i}) is included to describe anharmonicity in the pair distribution function.[8] If Δr_i becomes too large, $F_i(k)$ needs to be recalculated for a different value of r_i.

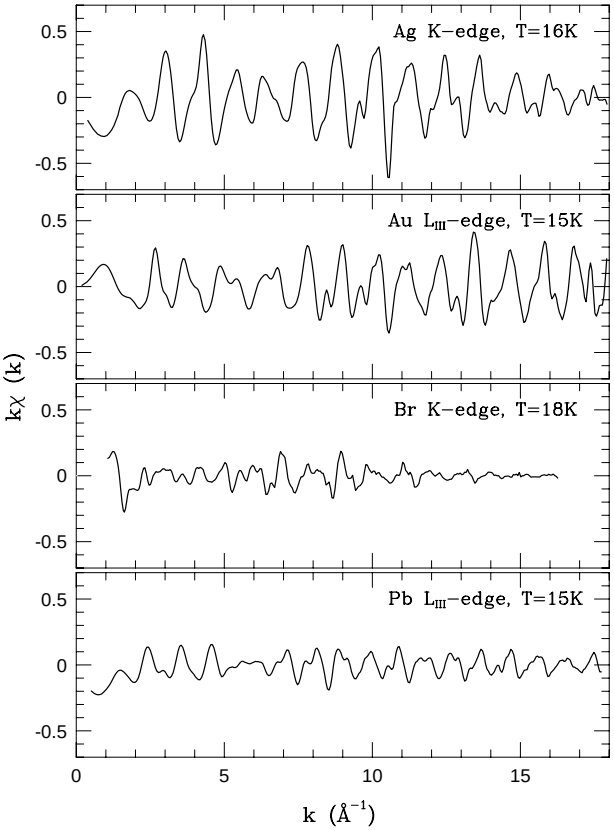

FIG. 1. Background subtracted data for all samples at low-temperature. Sample, edge, and temperature are indicated for each plot.

The Fourier transform (FT) of $\chi(k)$ into real (r) space is then taken using a Gaussian-rounded window with a width of 0.3Å to avoid transforming any sharp edges or discontinuities at the endpoints of the transform range. This produces a series of peaks in r-space corresponding to each shell of neighbors. The transform range is typically chosen to start around 2-3Å^{-1} (in k-space) and end when the EXAFS signal disappears into noise, anywhere from 12-18Å^{-1}. We use an automated process which varies the starting point of the spline-fit such that the Fourier transform at low r is minimized[4,6]. For data presented below, this range is typically 0-1Å.

In Fig. 1 we plot the k-space data for four edges at low temperatures. For the three metals, the XAFS oscillations extend above k = 17Å^{-1}, while for RbBr (Br K-edge) the XAFS oscillations are very small above 15Å^{-1}. The FT data for these k-space plots are shown in Fig. 2.

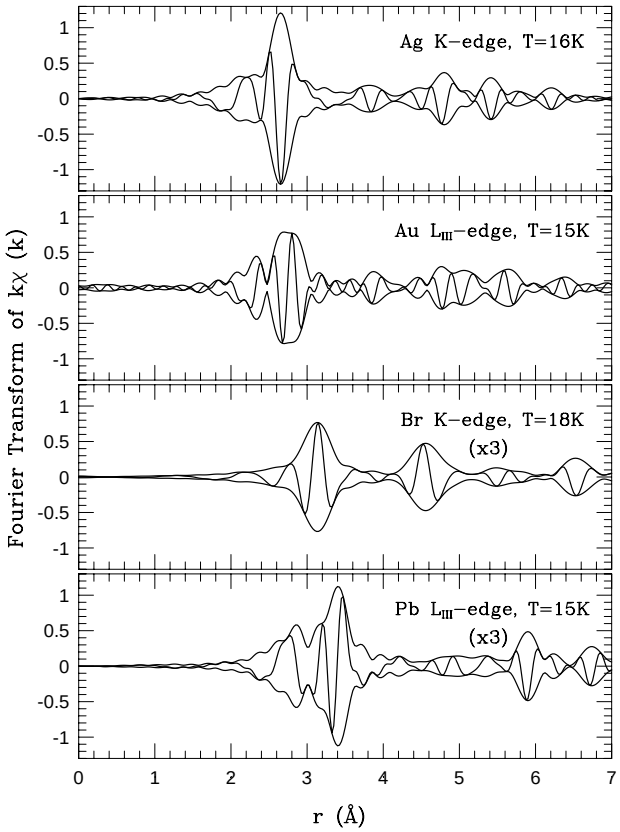

FIG. 2. Fourier transformed data for each sample at low temperature after an iterative background removal process. The k-space ranges used in the FT's are 3.1-16.5Å^{-1} for Ag, 3.4-16.8Å^{-1} for Au, 3.0-15.7Å^{-1} for Br, and 3.1-17.1Å^{-1} for Pb. Note also the degree of isolation of the first neighbor peak from further ones. The envelope function is given by ± [Re^2 + Im^2]$^{0.5}$ while the fast oscillation is the real part Re of the transform; Im is the imaginary part.

For all data presented here, the above steps alone could not produce an acceptably smooth transform in the region from 0-1.5Å, and an iterative background removal process was used[6]. In this method, the best background obtainable through the above methods is utilized, and theoretical FEFF standards are used to fit the data as well as possible. The best fit is then backtransformed and subtracted from the original data to yield a residue function. A better (trial) background function can then be created from the resulting residue function, which now

lacks most of its oscillatory behavior, and the new background can then be removed from the original data as before. This process requires 3-4 iterations before convergence to a reasonable background is achieved[6]. The backgrounds found through this process contain structure at low energies consistent with multi-electron excitations in the "Z+1" model[9] or atomic XAFS (AXAFS)[7]. They are also consistent with backgrounds extracted in other studies of the same edges[10]. Although we have used the iterative process to remove the structure below 1.5Å, there is essentially no change in the low-r side of the first FT peak above 2 Å between spline fits and the iterative background removal process (because the near-neighbor bond length is so long).

B. Fit Results

Fits were carried out in r-space for all neighbors up to about 6Å (including multi-scattering peaks). The Fourier transforms were fit using parameters ΔE_0, S_0^2, Δr, σ, and C_3. There are two sets of strongly correlated variables utilized in cumulant fitting : $\{\Delta r,\ \Delta E_0,\ C_3\}$ and $\{S_0^2,\ \sigma^2\}$. We assume that the pair distribution function is harmonic at the lowest temperatures for which we have data (15-20K), therefore higher cumulants ($n > 2$) are fixed at zero. For all fits presented here, low-temperature data were first fit to obtain values for ΔE_0 and S_0^2 while C_3 was fixed at zero. ΔE_0 and S_0^2 were subsequently held fixed for all fits (including those at higher temperatures). To avoid reliance on a single data trace, these values were obtained from the averages of the lowest two temperatures for each data set (15K-40K). The remaining parameters were then allowed to vary in order to obtain good fits. Since expansion is uniform in all directions for all these materials, the positions of all neighbors were constrained to vary such that the local structure remained consistent with a uniform cubic lattice. Single k-weighting ($k\chi$) was used in all transforms and fits.

Goodness of fit is measured by the quantity C^2, which measures the (square of the percentage) deviation between the theory and data.[4] It is proportional to a fractional χ^2. Although uncertainty in measurements can partially be estimated from the amplitude of the noise at high-k, estimates of errors on final parameter values are not easily obtainable. This is due in part to the use of Fourier transforms, which concentrate much of the noise above the fit range in r-space and to the subtraction of an unknown background function which introduces an unknown error. However, in many cases of interest here the unknown errors in the theoretical functions dominate. For these reasons, errors on parameter values are estimated by varying single parameters (in each direction away from the minimum) until $\sqrt{C^2}$ has doubled. The half-width of the resulting curve is then taken to be one standard deviation. This gives a very conservative estimate of errors, which are typically found by varying the parameter until χ^2 has doubled, or $\sqrt{C^2}$ reaches $\sqrt{2}$ times its minimum value.

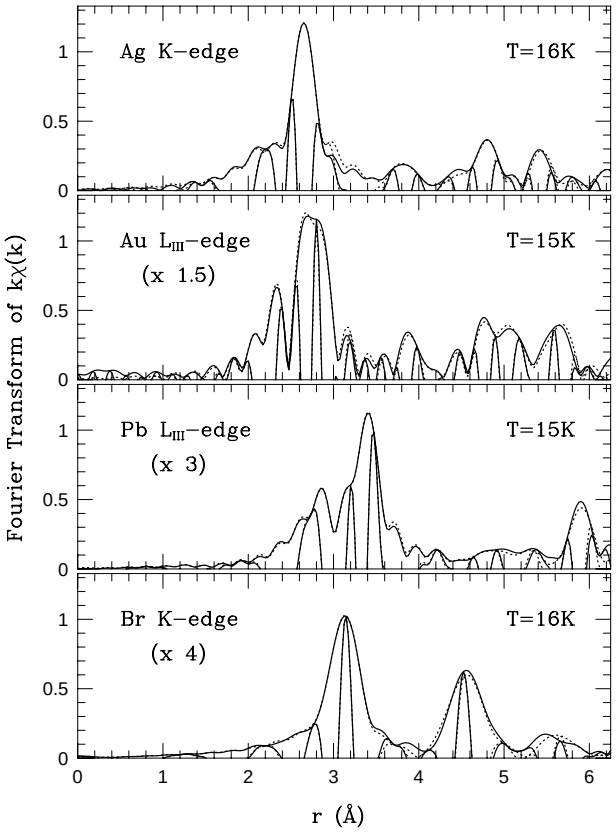

FIG. 3. FEFF fits (dotted lines) to low-temperature data over the first three (single-scattering) neighbors for Ag, Au, Pb, and Br as indicated in each plot. S_0^2 and ΔE_0 were found for each of these materials and fixed f or all further neighbors and higher temperature data. Shifts in position were constrained to be consistent with a uniform cubic lattice, and σ was allowed to vary for each neighbor.

Fit results for fits over both short and long ranges around the first neighbor peak are presented in Table II. These results are in good agreement with those found in similar analyses.[11] Differences in position seen for the first neighbor peak in fits over the two ranges were less than 0.002Å in all cases cited, so they are given only for the shorter range. (However note that because of correlations between r and E_o, and the fact that E_o may be shifted to account for disagreements in $F(k)$ between experiment and FEFF, the absolute errors on r are likely ± 0.005Å.) Other parameters are cited for both cases even though differences in most cases are small.

The most significant difference between equivalent fits over short and long ranges is in the goodness of fit, C^2, which can increase by more than a factor of five as a result of a 40% extension of the fit range. The reason for this is readily apparent in Fig. 3 where we plot transformed data along with fits using the FEFF6 standards. Although the fits are extremely good before and within the first neighbor peak, the amplitudes deviate consistently

on the high-r side of the first peak, where the FEFF calculations are consistently too large for the three metals studied, and too small for Br K-edge data. This effect is substantially more difficult to identify in further neighbors due to the presence of significant multiple-scattering peaks near and beyond the second neighbor, and the remainder of this paper will concentrate on the first neighbor only. It should be noted that in our initial fits of the data using only the FEFF functions, we have included the multiple scattering peaks out to 5.0 Å in generating the experimental standard. Many other multiple scattering paths do exist, but they produce FT peaks at even larger values of r and have no significant contribution in the vicinity of the first peak in r-space. Although most parameters are calculated automatically by FEFF, FEFF does allow several different exchange correlation potentials to be used (Hedin-Lunquist self-energy and the Dirac-Hara exchange correlation potential).[3] Each was tried with several values of the broadening parameters but none removed the problem on the high-r side of the first neighbor peak.

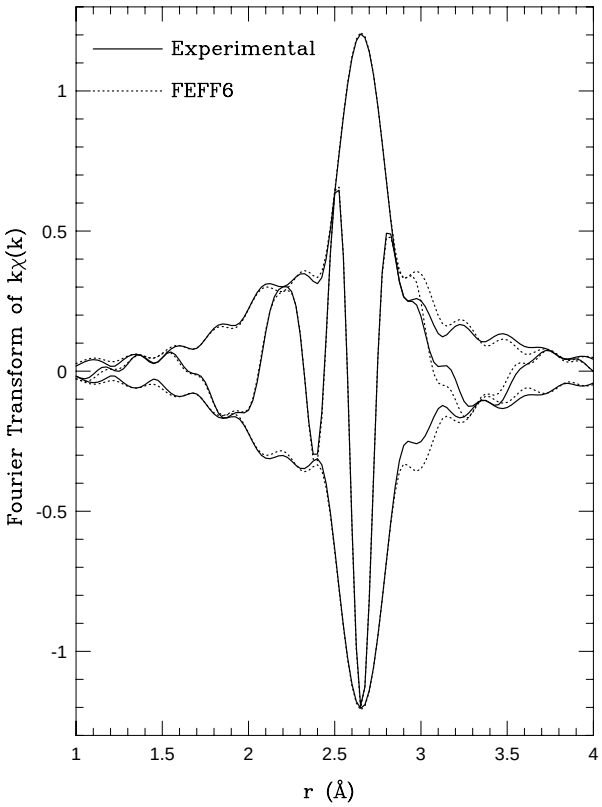

FIG. 4. Experimental standard extracted from T=16K Ag data, shown in solid. Dotted line shows the best FEFF standard fit to data. Same Ft range as in Fig 2.

C. Creating an Experimental Standard

As Fig. 3 shows (except for the deviations noted above), the fits are generally very good over the first few neighbors. This can be exploited to create an experimental standard from the transformed data. In Ref. 4 we have discussed the procedures for extracting an experimental standard and also provided a comparison between theoretical and experimental standards. The reader is referred to this paper for more details and other aspects such as transferring an experimental standard from one atom-pair to another. In that work we noted that there were important changes in the shape of the first neighbor peak but at the time did not recognize that the largest deviations always occurred on the high-r side of the peak, at least for all the systems we have studied.

For our studies of the Ag, Au, and Pb systems we have used the same approach to obtain a good experimental standard for determining changes in the local structure with temperature. These standards then simplify comparisons between FEFF and the data because the effects of more distant shells of neighbors have been removed.

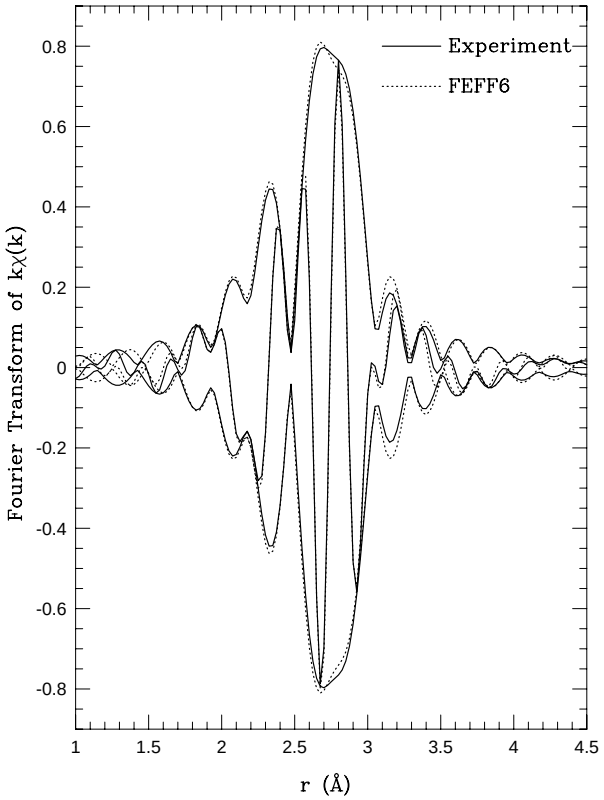

FIG. 5. Experimental standard extracted from T=15K Au data, shown in solid. Dotted line shows the best FEFF standard fit to data. Same Ft range as in Fig 2.

To make an experimental standard we take the best fit to the lowest temperature data using FEFF standards, and subtract the results for the further neighbors from the data set. This leaves the first peak essentially unchanged, with only the tails of the further neighbor peaks removed. As long as the fit quality is good for a significant distance around the first-neighbor peak, this file can be backtransformed over a suitable range to create an experimental (k-space) standard. Ideally this range is

chosen at points where the amplitude approaches zero, but we assume it suffices to choose endpoints where the amplitude decays to the level of noise in the data. For Ag, Au, and Pb, this was typically 3-4Å. For Br and Rb data, the fit was too poor over this wide a range to obtain a good experimental standard. This experimental reference is then used as the nearest neighbor peak standard in fits of the higher temperature data files for a given material.

In Figs. 4, 5, and 6 we compare the extracted and FEFF-generated standards for the nearest neighbor peak, to highlight the differences between them on the high-r side of the peak. The FEFF functions were refit to the experimental standard to minimize the differences.

IV. DISCUSSION

It should first be noted that when the experimental standards (Figs. 4-6) extracted from the low T data, are subsequently used to fit the remainder of the data (five data sets at temperatures between 20K and 293K for each material), the fits are superior even to those performed over a shortened range in r-space for the FEFF standard. The goodness of fit (C^2) for the first peak is typically improved by a factor of 4-10 when these standards are used, but can be much larger. The effect is very large for silver metal. Using an experimental Ag-Ag standard, extracted from the 16K data, a fit of the first peak for the 71K data, over the r-space range 2.0-3.3 Å gives C^2 of 0.5. In contrast using a FEFF6 standard for the same range yields $C^2 = 65.6$ (See Table II). In this case the improvement is more than 100 for this long fit range. Fig. 7 compares the best fits obtained with both FEFF and experimental standards to Ag K-edge data taken at 215K; again there is a large decrease in C^2 for the experimental standard - thus the deviations we observe are independent of temperature.

The FEFF-generated functions for the nearest neighbor shell consistently differ from the experimentally extracted ones on the high-r side of the transformed peak, where the FEFF amplitude is generally too large (metal foils) or too low (RbBr). Allowing parameters of the closest multiple-scattering peak to vary independently had no effect on this difference, nor did adding a fourth cumulant parameter C_4 to the fit. Note that there are no multiple-scattering peaks in the vicinity of the first neighbor peak; the only other contributions in this r-range arise from the small tails of peaks (both single and multiple scattering) that occur at longer distances. These small contributions were removed in generating the experimental standard.

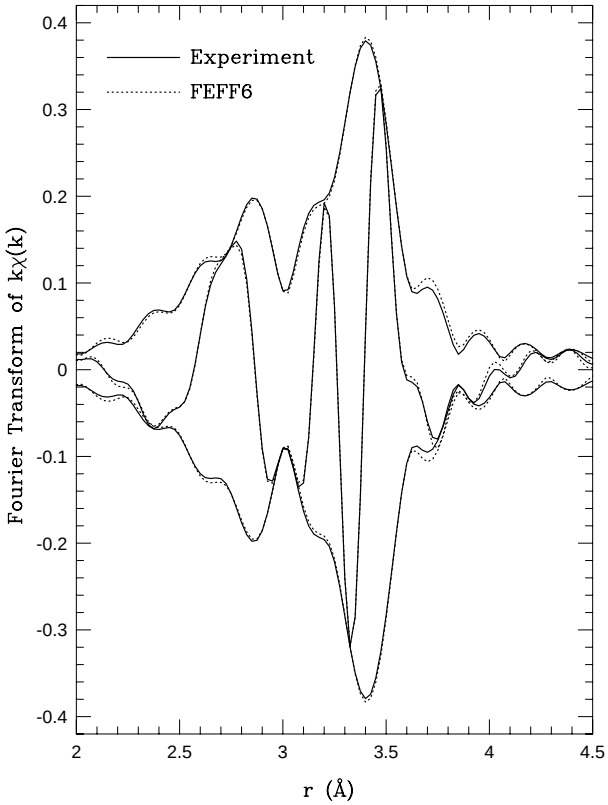

FIG. 6. Experimental standard extracted from T=15K Pb data, shown in solid. Dotted line shows the best FEFF standard fit to data. Same Ft range as in Fig 2.

To illustrate the problem that can arise when a distorted system is studied using FEFF generated standards, assume that the Ag data are really from some distorted crystal structure. Then one would expect possibly two or three different bond lengths. A fit to the first Ag shell using only one additional peak yields a very good fit but leads to the conclusion that there are roughly two Ag neighbors at a distance of 3.15 Å. For Ag this result is unphysical based on the well know structure of this FCC metal, but for an unknown system the error in the FEFF-generated standard (as a result of the approximations used) would lead to incorrect structural results. In Fig. 8 we compare the fits to the first peak in the Ag data using one or two FEFF standards. Clearly the two peak fit is much better. To quantify the improvement in the fit we determined C^2 for different r-space fit ranges 2-r_{end} Å (the fits are carried out in r-space). If the fit range is set at 2.0-2.8Å, we obtain an excellent fit with only one peak. As the fit range increases, C^2 increases rapidly for the single peak fit but increases slowly for the two peak fit as shown in Fig. 9; the number of Ag neighbors in the second peak changes from ~ 0 for the 2-2.8Å range to roughly 2 neighbors once the upper end of the range exceeds 3.0 Å.

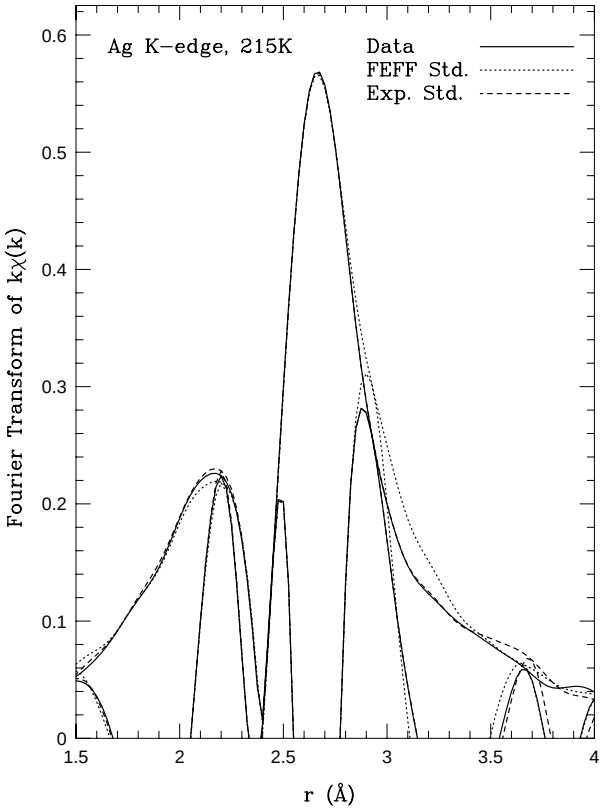

FIG. 7. Comparison of best fits to the first peak in the Ag K-edge data at 215K, over a fit range 2.0-3.3Å, using a FEFF6 standard (dotted line: $C^2 = 56$) and an experimental standard (dashed line: $C^2 = 1.2$). The latter was extracted from the 16K data. The data are plotted using a solid line.

In the case of Au, the change in C^2 for different fitting r-ranges (See Table II), is substantially smaller than for the other samples. The rather poor fit over most of the Au peak is responsible, although the greatest fit difference still remains on the high-r side of the peak. This can be seen more clearly if one re-plots the FEFF and experimental standards with all fit parameters "removed" from the data. Fig. 10 shows the experimental standard (transform), after removing ΔE_0, Δr, approximately removing σ, and normalizing by NS_0^2; it shows that the largest deviations relative to the FEFF calculations occur just above 3.0Å. However, Fig. 10 also illustrates another important aspect. There is a clear change in shape between Fig. 5 and Fig. 10; in Fig. 10 the agreement over the central part of the peak is excellent. For this case, most of the region where the data and FEFF differ has been shifted to high-r by the parameter ΔE_0. Because of the "shape change" introduced by ΔE_0 shifts, care must be taken when using this parameter as a variable with FEFF6 or FEFF7, since significant differences in shape can be introduced.

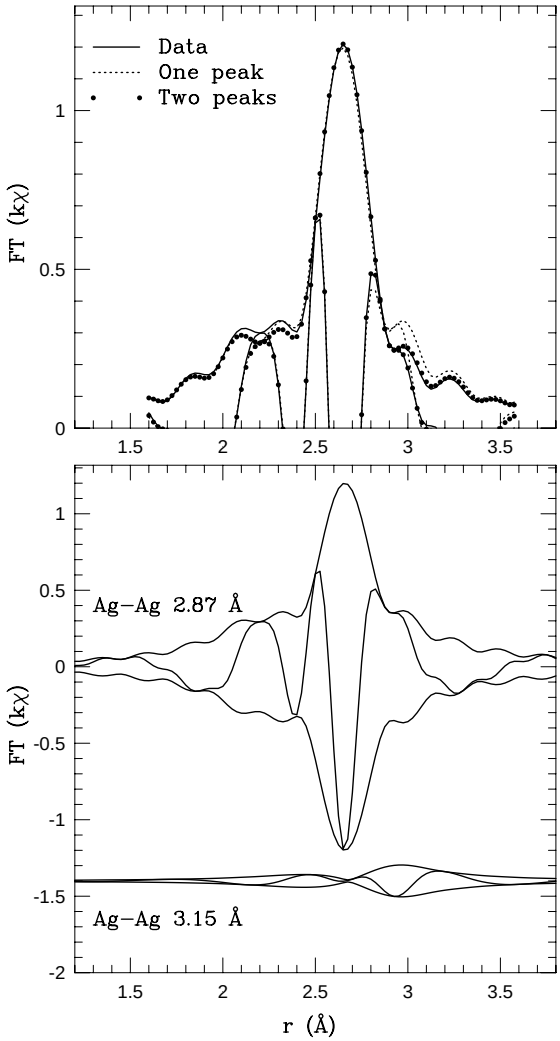

FIG. 8. A comparison of the single peak fit (dotted line) with the two peak fit (solid dots) for the first shell in Ag metal. Both FEFF standards are for Ag-Ag pairs. The individual peaks are shown separately in the lower part of the figure. The fit range for these fits is 2.0-3.4 Å.

To investigate the source of these discrepancies, we backtransformed from k to r-space and decomposed the EXAFS function into backscattering amplitude ($|F(k)|$) and phase ($\phi(k)$) functions, which are plotted in Fig. 11 and Fig. 12. The backscattering phases for the first neighbor calculated by FEFF are in remarkably good agreement with those extracted from the experimental standards. Nearly all disagreement arises in $|F(k)|$, as was also concluded in earlier studies.[4] While in rough agreement at high-k, the low-k portion of $|F(k)|$ is typically not in very good agreement with $F(k)$ calculated using FEFF. (However, note that when there is only a decreasing amplitude as is the case for Ag above 10 $Å^{-1}$, changes in the slope can be partially "corrected" by the value of σ obtained in the fit). For Pb, where the agreement between experiment and FEFF for F(k) is best, the amplitude problem in the transform is also very small.

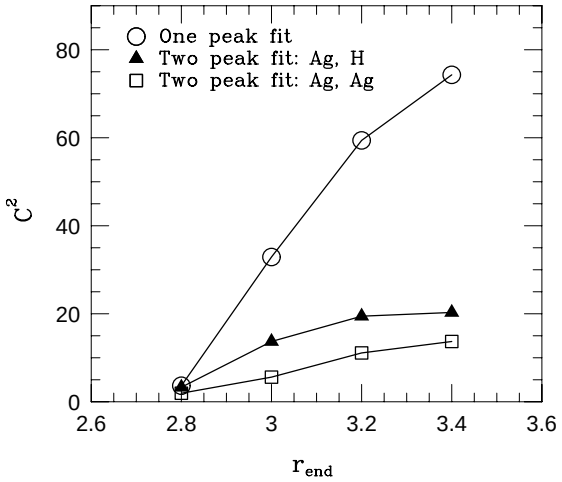

FIG. 9. C^2 as a function of the fit range in r-space, from 2Å to r_{end}Å. The circles show the rapid increase of C^2 when a single peak is used while the squares show the improved quality of fit using two Ag-Ag FEFF standards. The solid triangles show C^2 for fits which include interstitial H, as discussed below.

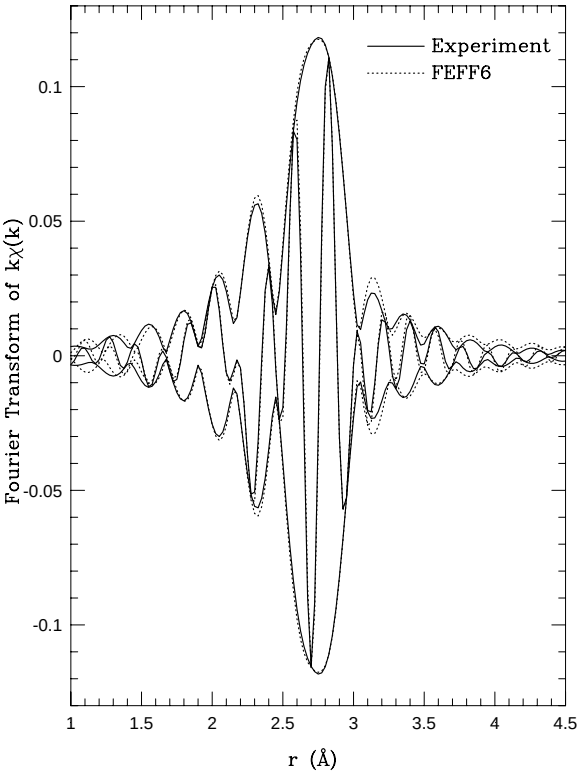

FIG. 10. Experimental standard (one neighbor) extracted from the low-temperature Au data, shown in solid. ΔE_0, Δr, σ, and NS_0^2 have been (approximately) removed. Dotted line shows FEFF6 standard for one neighbor, and is plotted exactly as generated from FEFF, with no Debye broadening.

For Ag and Au, where $F(k)$ from FEFF and $|F(k)|$ obtained by experiment disagree from about 4 to 8Å^{-1}, the discrepancy in the transforms is pronounced. Note the large deviation that occurs at the dip in $|F(k)|$ near 6Å^{-1}. The plot of $F(k)$ for Au also suggests why introducing $\Delta E_0 = -6.6eV$ has such a significant effect on the transform shape. Such an energy shift effectively displaces the (k-space) position of the structure in $F(k)$. Since the FT begins within the k-space region in which there is the largest discrepancy in $F(k)$ between FEFF and the data, shifting the position of the structure will change the FT.

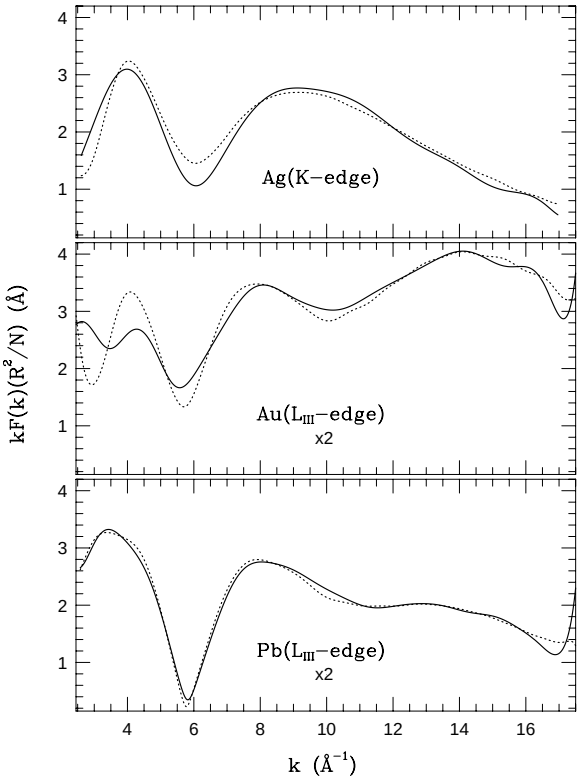

FIG. 11. Amplitude functions F(k) extracted from experimental standards (solid), and those generated by FEFF6 (dotted).

There are several possible explanations for these discrepancies. First, they may represent small errors as a result of various assumptions and approximations made in the atomic codes, for example, the treatment of the spin orbit coupling. If these are the dominant problems, the discrepancies should diminish as better models are developed. Very recent calculations by Rehr[12] using their most recent code (FEFF8.2) in which the spin orbit interaction is treated more accurately, improves the shape of the function for Au, but still did not significantly correct the problem for Ag. The systematic deviation on the high-r side of the peak suggests that some other aspect is missing in the calculations. One possibility is that part of the difference arise from additional scattering in the interstitial regions between "muffin-tin" atoms, particularly for the RbBr examples where an unexpected small peak occurs near 3.9Å, between the first and second neighbor peaks (See Fig. 3). It will also include

contributions from the difference between the spherical potential used for each atom in the muffin-tin model and the non-spherical atom potential in the real crystal. If scattering from these corrections to the potential are sufficiently large, it will produce peaks at unexpected distances, including new multiple scattering paths which combine regular atomic scattering with scattering from interstitial regions.

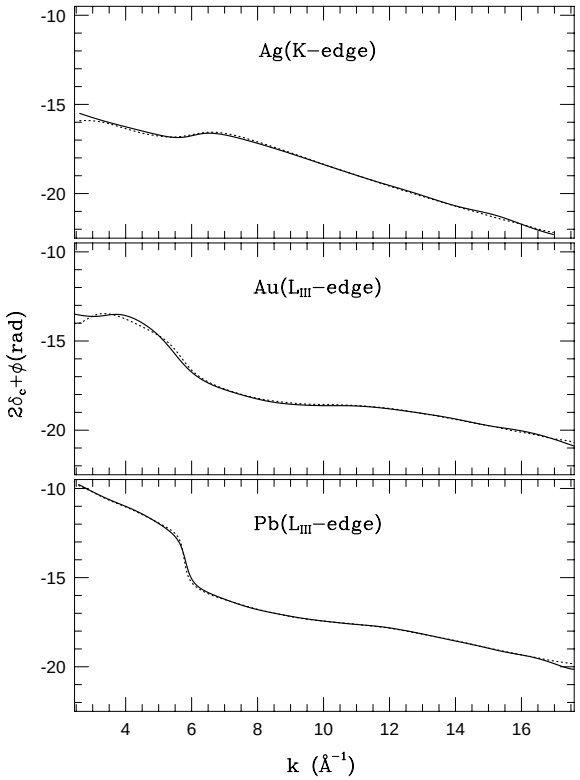

FIG. 12. Phase functions $\phi(k)$ extracted from experimental standards (solid) and those generated by FEFF6 (dotted).

There is growing evidence for atomic XAFS[7,13] (AXAFS) which arises from intra-atomic backscattering from the (partially interstitial) potential between two nearest neighbor atoms. It arises in the FEFF code as a result of partioning space into cells for each of the atoms in the material. Backscattering within the central atom cell (the intra-atomic backscattering) produces a modulation of the background function, μ_o; this modulation is called AXAFS. When muffin-tin discontinuities are minimized, the AXAFS obtained using the FEFF code, models experimental observations quite well (although a small amount of non-physical scattering from the muffin-tin potential discontinuities is still present). The structure presented here likely also involves intra-atomic scattering in the interstitial regions but unlike AXAFS it is scattering in more forward directions.

The real potential for the metals should have FCC symmetry rather than the spherical potential used in the muffin-tin model. To simulate this aspect we need additional interstitial scattering that is consistent with the lattice symmetry. To crudely model such interstitial scattering for Ag, we have added H atoms (i.e. one electron/H) at $\frac{a}{2}$ (a is the lattice constant) along each lattice direction and all equivalent positions (i.e. halfway between the center and second neighbor atoms) in the input file for FEFF to generate new scattering paths which include this small "interstitial" scattering effect. A new multiple scattering peak (with high multiplicity - 48) occurs just above the first neighbor peak, exactly where the discrepancy between FEFF and the data occurs. Note that these additional scattering contributions (central Ag atom-H-nearest neighbor Ag) would be included as part of the total first neighbor peak if nonspherical atom potentials were included in the calculations. An Ag-H-Ag standard was made for this path using the default options in FEFF. (The nearest neighbor Ag-H contribution turns out to be very small and is ignored.) Using FEFF7, the MT radius for H was 0.72 Å, while for FEFF6 it was 0.75 Å. As a first step, this multiple scattering contribution was just added to the Ag-Ag first neighbor standard, and a fit carried out without any additional adjustable parameters. This improved the fit which we take as evidence that these scattering paths are at least partly responsible for the observed discrepancy.

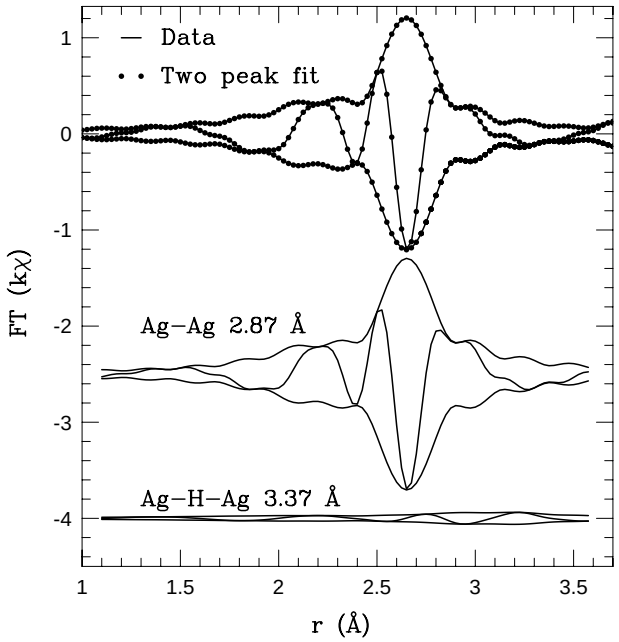

FIG. 13. A fit of the first shell for Ag metal to a sum of a Ag-Ag peak plus an Ag-H-Ag multiscattering peak for H at (a/2,0,0) and equivalent positions. The individual peaks are show n below.

To obtain better agreement (we don't know how much charge is neglected in the muffin-tin approximation) we used a sum of the Ag-Ag and Ag-H-Ag peaks over the r-space range 2-3.4 Å (for the 16K Ag data), with the parameters for each peak varied independently. Quite a good fit is obtained (See Fig. 13) with about 1.8 H at each interstitial position. C^2 decreases by a factor of 4

from the single FEFF6 peak fit as shown in Fig. 9. Since each H is also surrounded by 6 Ag atoms, this means that about 1.8 electrons/atom would contribute to this scattering process. However, to obtain a good fit the multiscattering path length (3.2Å) must be shortened by about 0.1Å.

To explore the effective number of electrons needed in this multi-scattering path we have compared FEFF6 and FEFF7 results and also used He (2 electrons) or Li (3 electrons) as the surrogate atom. We found in all cases that the number of electrons is close to 2; 1.7 for H with FEFF7 to 2.4 electrons for Li as the surrogate with FEFF6. Two electrons is higher than expected since Ag has one s-electron plus filled f and d shells. However, these low Z atoms are not really a good surrogate since the interstitial space is more like an "inverted" atom, with more electron density away from the site position, towards each Ag atom. (This may also account for the result that the fits always shortened the multi-scattering path length by .1-.2Å). An alternative approach would be to include empty spheres in the interstitial region (i.e. make a hole in the electron density by adding a positive potential energy term at the interstitial site)[14] and determine the scattering from them. Such calculations are not easily incorporated into FEFF and have not been attempted. Neither approach includes the non-sphericity of the interstitial region.

The low Z atoms included here do show that the resulting peak would occur in the region where the largest deviation between FEFF standards and the experimental data occurs. This indicates that in some cases scattering from the interstitial regions, which is neglected in MS calculations that use the muffin-tin or similar approximations, will produce additional structure on the high-r side of the first neighbor peak.

V. CONCLUSION

Although FEFF6.01a (and FEFF7.02) clearly produces very good EXAFS standards, there persist differences in the calculated backscattering amplitude function F(k) which can have important effects in EXAFS analyses. The systematic errors produced on the high-r side of transformed peaks may be more than a mere nuisance if the system under investigation is highly disordered or has dense atomic clusters with overlapping peaks, thereby making the source of the difference nearly impossible to isolate to a specific peak. There is some concern that differences of this order may even be mistaken for displaced atoms or imperfections, particularly when atoms are tightly clustered and S_0^2 is not well-known. For example, fits have shown that the high-r discrepancy in Ag can be fit quite well (with a significant decrease in C^2) if a few additional Ag atom defects are included at slightly greater distances than the first neighbor. However, this yields a local structure inconsistent with the known FCC structure.

In such cases, experimental standards are clearly preferable to those generated by the FEFF computer code. Ironically, nearest neighbor experimental standards are far easier to acquire when the FEFF-generated standards are also in reasonably good agreement with data for the further neighbor peaks. For RbBr, although the fit problems are similar to those found in Au, Ag, and Pb, the differences extend over a greater range such that they cannot be as easily isolated within a first-neighbor standard. Specifically, there is an extra small peak in the FT near $3.9 - 4.0$Å, roughly halfway between the first and second neighbor peaks. We have seen this feature in two different samples and it has appeared in the literature.[15] Lacking the ability to subtract the further neighbors properly from the data means that a high-quality nearest neighbor standard cannot easily be generated.

The presently available FEFF-generated standards should be considered to be very good approximations; excellent for a single first neighbor peak (in such cases the parameters are comparable using the experimental or FEFF standards). However, if a small peak overlaps the high-r shoulder of a large peak, significant problems can arise as discussed above. When using FEFF calculated functions to analyze EXAFS data, particularly disordered or distorted systems, one needs to evaluate whether such deviations bias interpretation of the results.

The deviation in the r-space region just above the first peak can be modeled by including some scattering from the interstitial region that is not included in the muffin-tin approximation. We have used low Z atoms (H, He,Li), located at the interstitial site half way between a Ag atom and it's second neighbor, as a surrogate for scattering in the interstitial region. This leads to a new, highly degenerate multiple-scattering path which produces a small broad peak exactly where the discrepancy occurs. Fits of the first peak in the Ag data to a sum of an Ag-Ag plus the multiple-scattering Ag-H-Ag peak were greatly improved. These fits suggest that roughly 2 electrons (i.e. two H atoms) are needed in this region to account for the observed structure in the r-space data.

It is important to eventually have theoretical functions that include most of the contributions from the crystal symmetry. We hope that the present work will stimulate better calculations that will include the local anisotropy about an atom and variations of the potential in the interstitial regions.

ACKNOWLEDGMENTS

We thank Professor J. Rehr, Matt Newville, and Corwin Booth for many helpful discussions and suggestions. The experiments were performed at the Daresbury Synchrotron Source in Daresbury, England. FB thanks the Daresbury Laboratory for their support while in Eng-

land. This work supported in part by NSF grant DMR-0071863.

[1] B. K. Teo, *EXAFS: Basic Principles and Data Analysis* (Springer-Verlag, New York, 1986).
[2] *X-Ray Absorption Principles Applications Techniques of EXAFS SEXAFS XANES*, edited by D. Koningsberger and R. Prins (Wiley, New York, 1988).
[3] S. I. Zabinsky, J. J. Rehr, A. Ankudinov, R. C. Albers, and M. J. Eller, Phys. Rev. B **52**, 2995 (1995).
[4] G. G. Li, F. Bridges, and C. H. Booth, Phys. Rev. B **52**, 6332 (1995).
[5] Z. Kvitky, Senior thesis, University of California, Santa Cruz, 1997.
[6] F. Bridges, C. H. Booth, and G. G. Li, Physica B **208&209**, 121 (1995).
[7] J. J. Rehr, C. H. Booth, F. Bridges, and S. I. Zabinsky, Phys. Rev. B **49**, 12347 (1994).
[8] G. Bunker, Nuclear Instruments and Methods **207**, 437 (1983).
[9] G. G. Li, F. Bridges, and G. S. Brown, Phys. Rev. Lett. **68**, 1609 (1992).
[10] A. Filipponi and A. Di Cicco, Phys. Rev. A **52**, 1072 (1995).
[11] M. Newville, Ph.D. thesis, University of Washington, 1995.
[12] J. Rehr, Private communication.
[13] H. Wende, Ph.D. thesis, Free University Berlin, 1999.
[14] J. Keller, J. Phys. C **4**, L85 (1971); **4** 3143 (1971).
[15] A. I. Frenkel, E. A. Stern, M. Qian, and M. Newville, Phys. Rev. B **48**, 12449 (1993).

TABLE I. Energy resolution for each data set based on the tabulated edge energy (E_0) and slit height.

Sample	E_0 (keV)	Slit Height (mm)	Resolution (eV)
Ag K	25.523	0.3	4
Au LIII	11.921	0.7	2
Br K	13.475	0.7	2
Pb LIII	13.043	0.7	2

TABLE II. S_0^2 is an amplitude reduction factor, ΔE_0 is a shift in edge energy, R is the distance to the nearest neighbor, σ^2 is the Debye-Waller factor, C_3 is the third cumulant, and C^2 quantifies goodness of fit. Error estimates for each parameter (one-parameter uncertainties) are given in parentheses, indicating the error in the last significant digit(s). All values of S_0^2 and ΔE_0 were fit at low temperatures and held fixed for higher temperature data. Results are given for fits using FEFF6 standards over short and long ranges in r-space. The units for σ are 10^{-2}Å and for C_3, 10^{-5}Å^3.

				short range					long range				
Edge	T(K)	R (Å)	ΔE_0	Range	S_0^2	σ	C_3	C^2	Range	S_0^2	σ	C_3	C^2
Ag	16	2.871(2)	-3.4(4)	2.0-2.9	0.96(3)	4.6(2)	0.	15.2	2.0-3.3	0.92(5)	4.1(5)	0.	64.0
	71	2.872(2)				5.3(2)	0.	11.6			4.9(4)	0.	65.6
Au	15	2.878(2)	-6.6(6)	1.9-3.1	0.86(3)	3.3(2)	0.	21.2	1.9-3.3	0.85(3)	3.2(3)	0.	29.2
	114	2.879(3)				5.2(2)	1(3)	22.1			5.2(2)	0.	30.3
Br	18	3.416(1)	-1.3(2)	2.4-3.4	0.93(1)	6.9(1)	1(4)	5.3	2.4-3.8	0.94(3)	6.8(2)	3(9)	16.8
	81	3.421(2)				8.7(1)	10(3)	6.3			8.6(3)	10(9)	36.0
Pb	15	3.475(1)	1.7(1)	2.4-3.6	0.89(1)	5.3(1)	1.5(8)	3.2	2.4-4.1	0.87(2)	5.3(1)	0.	10.2
	88	3.485(2)				9.5(1)	21(4)	10.9			9.5(3)	19(8)	19.4